

12

Fundamental cloud dynamics

In the discussions of cloud microphysical processes, we have implicitly assumed that the dynamical and thermodynamic environments remain unchanged. In reality, cloud microphysical processes are closely coupled with dynamics and thermodynamics, such that changes in cloud microphysics will lead to changes in cloud dynamics and thermodynamics, and vice versa. For example, a phase change of water substance will cause the release or consumption of latent heat, which will heat or cool the surrounding air and eventually lead to air motion. The formation of large hydrometeors such as raindrops or hail increases the downward drag of the air parcel they are in and thus may cause the air to descend. The ascent or descent of air causes cooling or heating due to adiabatic expansion or compression, and may lead to the formation or dissipation of hydrometeors.

To really take these interactions into account, we need to develop a cloud model that includes the coupled dynamical, thermodynamic, and microphysical processes. We will discuss the cloud models in the next chapter, but it is useful to review some key dynamical processes of cloud development in a simplified setting so as to understand the fundamental processes involved. This is the subject of this chapter.

12.1 Cloud motions

Before we discuss the basic cloud dynamics, let us try to clear up a common misunderstanding that many casual cloud watchers may have. It is our common experience to see a small puffy cumulus floating in air against the blue sky and the cloud sometimes moves in a certain direction. Our intuition would be that the cloud moves with the wind. Is that true? The answer is “no”! It is the air that is moving, and the cloud forms in the air. The moving speed of the cloud may or may not be the same as the air speed. In some cases, such as the wave clouds that form in the lee of a mountain, the clouds often appear to be stationary but the air moves rapidly! Fig. 12.1 shows two frames of wave clouds taken from a video dated 16 August 2007

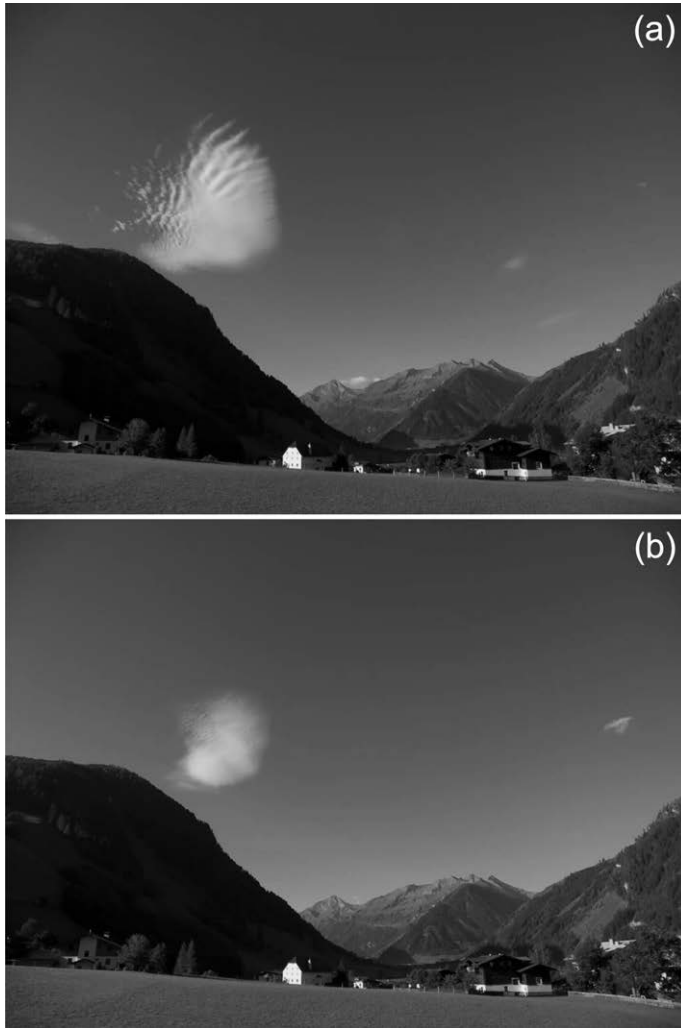


Fig. 12.1 Mountain wave cloud formation at Rauris Valley (Raurisertal) in Hohe Tauern National Park, Salzburgerland, Austria, on 16 August 2007. Frames (a) and (b) were separated by about 30 min. The wind was blowing, but the cloud appears to be stationary. The video is available at <http://www.setvak.cz/timelapse/2007.html>. Courtesy of Dr Martin Setvák.

(available at <http://www.setvak.cz/timelapse/2007.html>). The two frames were taken 30 min apart. By watching the video, it is clear that there were winds but the cloud in the center left of the picture appears to stay in the same place, although its shape has changed. What actually happened was that the wind blew across the mountain and produced mountain waves. The wave motion at the location where this cloud appeared is such that it is favorable for cloud formation. When water vapor carried

by winds arrives here, condensation occurs and cloud appears. But when cloud particles (also carried by winds) pass this position, they evaporate because of unfavorable conditions and the cloud disappears. But new air with water vapor keeps coming and condensation keeps occurring at the same location, and that gives the illusion that the “cloud” is always there.

When we watch these time-lapse cloud videos, we sometimes see that the clouds literally “disappear before our eyes”, and sometimes “appear from nowhere”. It is clear that we are not seeing the motion of an object, such as a solid ball that does not change its content during its motion. Rather, a cloud is an ensemble of gases (air, water vapor, etc.) and condensates (liquid drops, ice particles). These condensates, and hence the cloud, may appear or disappear depending on the environmental conditions, and what we are seeing as the “cloud” entity is the motion of the “pattern” of the cloud, not the cloud particles.

The so-called “touch-down” of a tornado funnel is of similar nature. The funnel is made of water drops due to the rapid expansion of air in the funnel, so it is essentially a cloud. The air in the funnel is going up rapidly, as can sometimes be visualized from the motions of debris in it, yet the funnel seems to be lowering from above during the touch-down. In reality, it is the “pattern” of the funnel that is coming down but the particles in it are going up! The pattern seems to come down because the condensation at higher level forms first and that in the lower levels forms later. The “time sequence of condensation” produces the illusion that the funnel cloud lowers from above.

In a sense, cloud motion is akin to (though not really equivalent to) the propagation of waves. The wave pattern (phase) moves with the phase speed but the medium where the waves occur may not be moving at all.

12.2 Adiabatic ascent of an unsaturated air parcel

The most common process of cloud formation in our atmosphere is adiabatic cooling, as we have derived in Sec. 4.4. There we started out by assuming that an unsaturated air parcel that is rising adiabatically will cool down at the dry adiabatic lapse rate of $\sim 9.76 \text{ K km}^{-1}$, or roughly 10 K km^{-1} . The rate would change slightly if there were water vapor in the air parcel, but the magnitude is small enough to be negligible for the possible amount of water vapor in air as long as the air is unsaturated.

Note that, since $dQ = TdS = 0$ during an adiabatic process, the entropy S of the parcel is conserved. Hence an adiabatic process is also called an isentropic process. In atmospheric science, it is common to use the *potential temperature* θ to represent the conserved quantity during this process instead of entropy, θ being defined as

$$\theta = T \left(\frac{P_0}{P} \right)^\kappa, \quad \kappa = \left(\frac{R_d}{c_p} \right) = 0.286, \quad (12.1)$$

and the reference pressure P_0 is taken as 1000 mb (or 100 hPa). Thus the potential temperature is the temperature the air parcel would have if it were displaced from anywhere to 1000 mb via an adiabatic process, and it remains constant during this process. In simplified theoretical studies, atmospheric processes are often assumed to be adiabatic and the potential temperature can be used as a “tracer” to keep track of the movements of air parcels. This is especially useful to atmospheric chemistry, where the source origin of certain species is of central importance.

12.2.1 Lifting condensation level

We see that, as the parcel rises adiabatically, it expands and cools at a rate of 9.76 K km^{-1} . As the air parcel cools, the water vapor in the air parcel becomes closer to saturation because the saturation vapor pressure decreases with decreasing temperature. As the air parcel rises high enough, it will eventually reach a level at which its temperature becomes cold enough to saturate the vapor, and any further ascent (hence cooling) will cause excess water vapor to condense – and we will start to see cloud appearing! The level where the air parcel becomes saturated due to adiabatic ascent is called the *lifting condensation level* (LCL). The LCL can be determined graphically from adiabatic charts (such as the so-called skew- T log- P chart) for a specific sounding. Many elementary textbooks of meteorology contain discussions of these adiabatic charts.

Further ascent of the air parcel above the LCL would cause more condensation as long as there is still excess water vapor in the parcel and hence further cloud growth. But the thermodynamic process in this stage is no longer dry adiabatic because the release of latent heat due to the phase change of water begins to influence the temperature of the air parcel. We need to examine this more quantitatively.

12.3 Moist adiabatic process

The formation of condensed water in clouds introduces complications into the thermodynamics. To a first approximation, we will consider a moisture-containing air parcel that reaches saturation but retains all the condensed water and the latent heat released within the parcel. If the parcel descends, then we assume that water drops or ice particles will evaporate and latent heat is consumed, but again all materials and energy remain in the parcel. In other words, this system is thermodynamically reversible and also isentropic. This thermodynamic process is called the *reversible moist adiabatic process*.

While it is conceptually simple, this reversible process is cumbersome to apply because the air parcel must now carry the condensed water along during its ascent or descent, which makes the calculation of energy balance very complicated. A common practice to simplify the situation is to assume that all the condensed water falls out of the parcel as soon as it is formed but carries no energy away. Since the amount of energy carried by condensed water is mostly negligible compared to that of the air parcel, at least for the case of small cloud formation, this assumption is acceptable as a first approximation, and we can conduct our calculations as if the air parcel were still undergoing an adiabatic process. This process is called the *pseudo-adiabatic process* and is the basis of the following discussion.

Now let us examine how the temperature lapse rate of this pseudo-adiabatic system differs from that of a dry adiabatic system. For simplicity, we will just consider the condensation of water drops and ignore the ice phase, as the ice process is analogous. Thus, when the air parcel reaches the LCL, the water vapor is saturated, latent heat is released, and adiabatic energy conservation requires that, instead of (4.2), we should have

$$c_{p,m}dT + L_e dq_{v,\text{sat}} - \alpha_m dp = 0, \quad (12.2)$$

where $q_{v,\text{sat}}$ is the saturation mixing ratio of water vapor, $c_{p,m}$ is the specific heat, and α_m is the specific volume of the moist air. Unlike the case of dry air, the latter two quantities are not constant because they depend on how much water vapor there is in the parcel, i.e. they are a function of $q_{v,\text{sat}}$. Expressing these quantities explicitly and using the ideal gas law for the third term, we rewrite (12.2) as

$$(c_{p,a} + q_{v,\text{sat}}c_{p,v})dT + L_e dq_{v,\text{sat}} - (R_a + q_{v,\text{sat}}R_v)T \frac{dp}{p} = 0. \quad (12.3)$$

The terms with “v” subscript represent that quantity for water vapor and those with “a” subscript those for dry air. Here the first term represents the energy due to the change of parcel temperature dT (measured at constant pressure), the second term the latent heat released, and the third term the change due to the change in pressure. Note that we have completely ignored the heat carried away by the water drops that fall out of the air parcel, which is very small anyway.

We further simplify (12.3) by noting that the vapor-related quantities in the first and third terms are small compared to the dry air quantities and hence can be ignored. Thus, after rearrangement, we have a new approximation:

$$c_{p,a} \frac{dT}{T} + L_e \frac{dq_{v,\text{sat}}}{T} - R_a \frac{dp}{p} = 0. \quad (12.4)$$

Following the same procedure as in Sec. 4.4, we obtain the temperature lapse rate of the moist air parcel as

$$\Gamma_s = -\frac{dT}{dz} = \frac{g}{c_{p,a} + L_e(dq_{v,\text{sat}}/dT)}. \quad (12.5)$$

This is called the *pseudo-adiabatic lapse rate*. Since all quantities on the right-hand side of (12.5) are positive, we immediately see that this lapse rate is always smaller than the dry adiabatic lapse rate (4.8), i.e. $\Gamma_s < \Gamma_d$. Secondly, the pseudo-adiabatic lapse rate is not constant but depends on $dq_{v,\text{sat}}/dT$, the amount of water vapor condensed due to cooling. Typical values of Γ_s range from $\sim 4 \text{ K km}^{-1}$ (lower troposphere) to $\sim 7 \text{ K km}^{-1}$ (upper troposphere).

During a pseudo-adiabatic process, the potential temperature θ is no longer conserved because the latent heat effect is not included in the definition of the potential temperature (12.1). However, it is possible to include this effect by defining another quantity, the *equivalent potential temperature* θ_e , which will be conserved during a pseudo-adiabatic process:

$$\theta_e = \left(T + \frac{L_e q_v}{c_p}\right) \left(\frac{P_0}{P}\right)^\kappa = T_e \left(\frac{P_0}{P}\right)^\kappa, \quad (12.6)$$

where q_v is the mixing ratio of water vapor and T_e as defined above is called the equivalent temperature. Thus the equivalent potential temperature can be used as a tracer during a pseudo-adiabatic process.

12.4 Buoyancy and static stability

It is usually assumed that, as soon as an air parcel rises to a certain level, its pressure will immediately be balanced with that of its surrounding environment. In reality, of course, it always takes a finite amount of time to do so, but this is a good approximation, as there is not really a rigid boundary between them. At the same pressure, an air parcel will be lighter than its environment if it is warmer, and the parcel will be subject to a buoyant force defined by

$$F_B = mg \left(\frac{\rho - \rho'}{\rho'}\right) = mg \left(\frac{T - T'}{T'}\right) = mg \left(\frac{\theta - \theta'}{\theta'}\right), \quad (12.7)$$

where the primed quantities are that of the environment. In this case, the parcel will rise due to the buoyancy. If, on the other hand, the parcel is colder than its environment, then it will be subject to a negative buoyant force and sink.

Since the formation of clouds is usually related to the ascending motion of air, the static stability of air in which clouds form plays an important role. When an air parcel, which was originally in thermal equilibrium with its environment (so that the two have

the same temperature), is displaced vertically by a perturbation from its initial position (either upward or downward), it is the static stability of its environment that decides the parcel's reaction. If the parcel continues to accelerate away from its initial position, then its environment is unstable. If, instead, the parcel moves back to its initial position, then its environment is stable. Obviously, there is a third condition that sits right between the stable and unstable conditions – the neutral condition, where the parcel moves at a constant speed (no acceleration) and in the direction caused by the perturbation. If the motion of the air parcel is adiabatic, then the static stability condition of its environment is determined by the relative magnitude between the environmental temperature lapse rate and the adiabatic lapse rate according to the following relations:

$$\left. \begin{array}{l} \Gamma < \Gamma_d \text{ stable} \\ \Gamma = \Gamma_d \text{ neutral} \\ \Gamma > \Gamma_d \text{ unstable} \end{array} \right\} \text{unsaturated} \quad \text{or} \quad \left. \begin{array}{l} \Gamma < \Gamma_s \text{ stable} \\ \Gamma = \Gamma_s \text{ neutral} \\ \Gamma > \Gamma_s \text{ unstable} \end{array} \right\} \text{saturated.} \quad (12.8)$$

Remember, of course, that Γ_s is not a constant and $\Gamma_s < \Gamma_d$. Now it may happen that the environmental lapse rate Γ is such that $\Gamma_s < \Gamma < \Gamma_d$, then clearly the stability depends on whether the air parcel is saturated or subsaturated. This situation is called *conditional instability*.

The stability conditions can also be expressed in terms of the potential temperatures. From (12.1) we have

$$\ln \theta = \ln T + \kappa \ln p_0 - \kappa \ln p$$

and therefore

$$\begin{aligned} \frac{1}{\theta} \frac{d\theta}{dz} &= \frac{1}{T} \frac{dT}{dz} - \frac{\kappa}{p} \frac{dp}{dz} = \frac{1}{T} \frac{dT}{dz} + \frac{(R_d/c_p)}{\rho_a R_d T} (\rho_a g) \\ &= \frac{1}{T} \left(\frac{g}{c_p} + \frac{dT}{dz} \right) = \frac{1}{T} (\Gamma_d - \Gamma), \end{aligned} \quad (12.9)$$

after applying the hydrostatic balance equation and the ideal gas law. Thus

$$\frac{d\theta}{dz} = \frac{\theta}{T} (\Gamma_d - \Gamma). \quad (12.10)$$

Using (12.8) and (12.10), we can express the stability condition in terms of the potential temperature as

$$\left. \begin{array}{l} \frac{d\theta}{dz} > 0 \text{ stable} \\ \frac{d\theta}{dz} = 0 \text{ neutral} \\ \frac{d\theta}{dz} < 0 \text{ unstable} \end{array} \right\} \text{unsaturated} \quad \text{or} \quad \left. \begin{array}{l} \frac{d\theta_e}{dz} > 0 \text{ stable} \\ \frac{d\theta_e}{dz} = 0 \text{ neutral} \\ \frac{d\theta_e}{dz} < 0 \text{ unstable} \end{array} \right\} \text{saturated.} \quad (12.11)$$

12.5 The adiabatic parcel model of cloud formation

We can now form a conceptual model of cloud development based on the assumption that all processes are dry adiabatic before saturation or pseudo-adiabatic after saturation of the air parcel. We further assume that the parcel motion does not disturb its environment. This is called the *parcel model*. When such an air parcel rises, it expands and initially cools at a rate equal to Γ_d . Eventually, the parcel rises to the height of the LCL. Here, the air inside the parcel becomes saturated, condensation starts, and a cloud begins to appear. Now latent heat is released, the parcel continues to rise (since it still has positive buoyancy), and cools according to Γ_s , and more condensation (hence a taller cloud) occurs if excess water vapor is still available. This continues as long as the parcel is still warmer, hence lighter, than its environment. Eventually, the parcel may reach a level where its temperature is the same as that of the environment. The level at which the parcel and its environment have the same temperature is called the *level of neutral buoyancy* (LNB) or the *equilibrium level* (EL) because the parcel loses its buoyancy here.

However, the parcel will not come to a complete halt at the LNB because it still has kinetic energy. Instead, it will continue to rise until it expends all the kinetic energy. The height that the parcel rises above the LNB is called the *overshooting*. In the case of severe thunderstorms, where the LNB is often located at the tropopause, the overshooting represents a part of the cloud that protrudes into the stratospheric level (but see Chapter 13 for a clarification of what this implies) and is often called the *overshooting top* or *overshooting dome* because of its dome shape (Fig. 12.2).



Fig. 12.2 The overshooting top of a thundercloud over Utah on 18 July 2008 as seen from an aircraft flying at the tropopause level. Photo by Pao K. Wang.

For smaller cumulus congestus or cumulonimbus, however, the overshooting may occur entirely in the troposphere.

12.5.1 Convection condensation level

Using the adiabatic ascent idea described above, we can form a simple conceptual model of convective cloud formation. Fig. 12.3 shows a possible scenario of the evolution of a sounding on a typical summer day. In the early morning, the

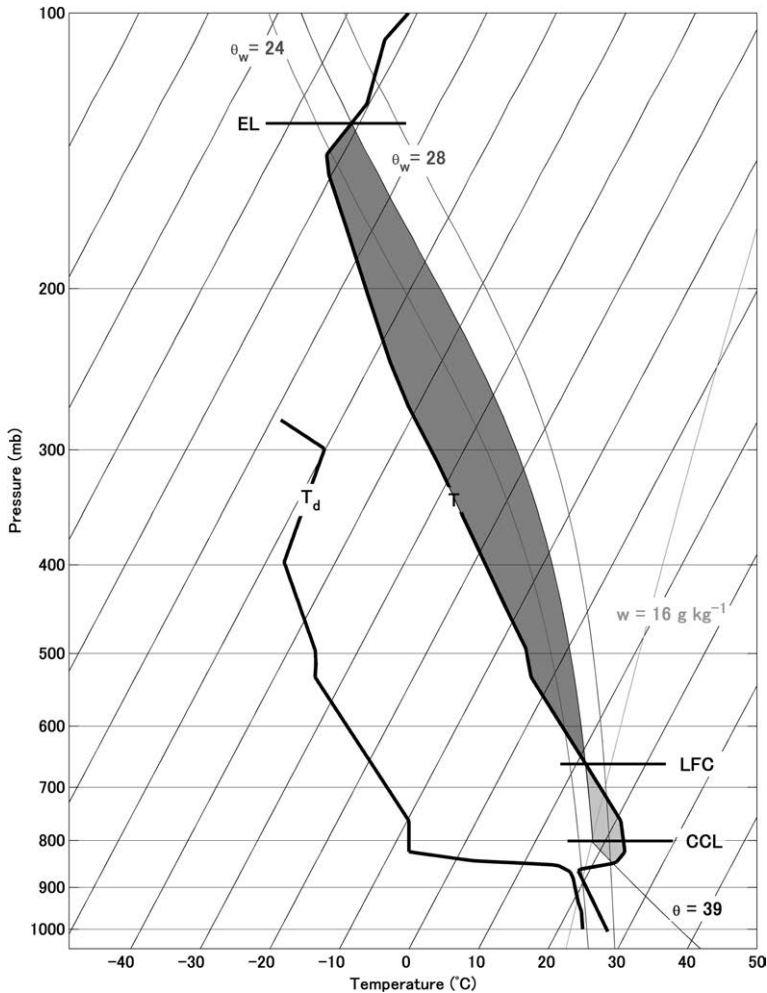


Fig. 12.3 A typical sounding favorable for the formation of a severe convective storm in the Great Plains region of the USA. The dark shaded area above ~ 650 mb represents the convective available potential energy (CAPE) and the lighter shaded area between ~ 950 and ~ 650 mb represents the convective inhibition (CIN). Adapted from Doswell (2001).

temperature sounding curve shows a shallow inversion near the ground due to the overnight radiative cooling. When the Sun is out, the surface starts to receive heat and the temperature of the lower-level air increases by conduction from the surface and by mixing in the air. The mixing homogenizes the water mixing ratio of the low-level air and essentially brings the moist boundary layer air upward, forming the mixing layer. The mixing layer continues to grow as the morning becomes later and eventually a temperature T_c on the surface is reached some time in mid-morning. Using the adiabatic chart, we see that (assuming that the mixing ratio of water vapor remains constant), at this time, a parcel on the surface that rises adiabatically would reach a level at which the T curve intersects the mixing ratio (w_v) curve, where condensation should occur and we can expect to see the formation of a cumulus. This level is called the *convective condensation level* (CCL). The cumulus will continue to grow if the layer above the CCL is moist unstable.

The above scenario provides a way to forecast the cumulus cloud base height if the convective surface temperature can be predicted. In many typical convective cloud cases, the CCL is very close to the LCL mentioned previously.

12.6 Corrections to the parcel model

12.6.1 Burden of condensed water

In the above discussions, we assumed that the parcel rises according to the pseudo-adiabatic theory and we did not consider the impact of the weight of the condensed water on the motion of the parcel. After the parcel reaches the LCL, condensed water forms and its weight becomes a burden (downward force) or drag on the parcel that will impede its buoyancy. Therefore, instead of (12.7), the net force acting on the parcel should be

$$F_B = mg \left(\frac{T - T'}{T'} \right) - m_{\text{con}} g = mg \left(\frac{T - T'}{T'} - \frac{m_{\text{con}}}{m} \right) = mg \left(\frac{T - T'}{T'} - q_{\text{con}} \right), \quad (12.12)$$

where m_{con} and q_{con} represent the mass and mixing ratio of the condensed water in the parcel. Eq. (12.12) implies that the parcel will not rise as fast as in the no-burden case.

12.6.2 Adiabatic slice model – a first correction to the test parcel model

While the test parcel model gives us useful insights into the cloud formation process, it is admittedly a crude first approximation. Several important processes are not considered by this model, the two most important of which, namely dynamic

coupling and mixing with the environment, both impact significantly on cloud development. These processes will be discussed briefly in the following sections. More detailed discussions of them can be found in Scorer (1997) and Iribarne and Godson (1973).

12.6.3 Dynamic coupling of the parcel and the environment

Since the air is a continuous fluid, when there are updrafts in a region of air that was initially at rest, there must be compensating downdrafts somewhere else in that region. This is the case when a thermal rises. The rising motion of the thermal would therefore cause the air around it to make a compensating descent. This is proven by aircraft observation of vertical air velocity around a developing cumulus, as shown in Fig. 12.4.

Here we see that the positive liquid water content region in the lower panel corresponds to the cloudy air formed by the thermal. The vertical velocity profile in the upper panel shows that there are updrafts in the cloud, whereas the regions immediately outside of the cloud edge are dominated by downdrafts, which are the compensating downward motions of the updrafts.

Now, since the environmental air is subsaturated, its downward motion will cause it to heat up by dry adiabatic compression. Its initial temperature profile

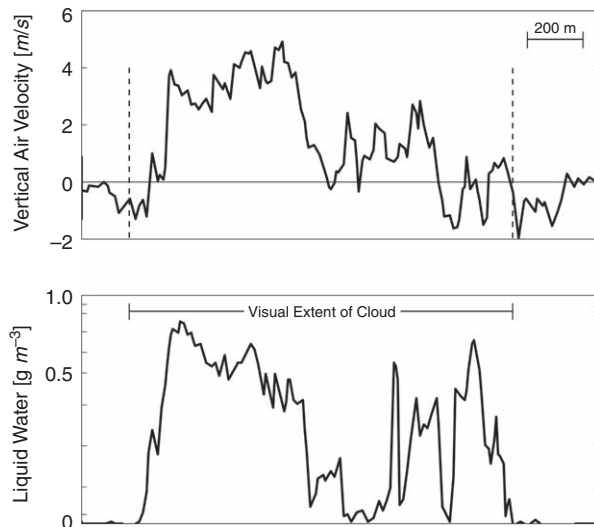


Fig. 12.4 Relation between updraft and liquid water content from an aircraft penetration of a cumulus cloud. The horizontal axis represents the horizontal distance. The two vertical dashed lines in the upper panel denote the cloud boundary. Adapted from Warner (1969).

and hence the static stability will be altered. This change can be estimated by the slice method (also called layer method). We will call it the *slice model* here. The main idea is that, as a result of continuity, the total mass flux due to the compensating downdrafts should be the same as the mass flux of the air parcel:

$$\rho A w = \rho' A' w', \quad (12.13)$$

where ρ , A , and w are the density, horizontal cross-sectional area, and vertical velocity of the parcel, and the prime indicates the corresponding quantities of the environment. Thus the compensating downdraft can be estimated by

$$\frac{w'}{w} = \frac{\rho A}{\rho' A'} \approx \frac{A}{A'}. \quad (12.14)$$

Thus the impact depends on the ratio of the cross-sectional areas. If the parcel area is very small, i.e. $A \rightarrow 0$, then the parcel motion has nearly no impact on the environment. If instead A is substantial, then the induced downdraft w' is also substantial.

Now suppose that the parcel ascends and cools at the pseudo-adiabatic lapse rate, whereas the surrounding environment descends and warms up at the dry adiabatic lapse rate. Thus, in a short time dt , the parcel with initial temperature T_0 that ascends to a new level will have a temperature $T = (T_0 + \Gamma w dt) - \Gamma_s w dt$, whereas the environmental air that descends to this level will have a temperature $T' = (T_0 - \Gamma w' dt) + \Gamma_d w' dt$, where the quantities in the parentheses are the temperatures of the parcel and the environmental air at their respective initial level. The difference between the two temperatures is

$$\Delta T = T - T' = (\Gamma - \Gamma_s)w - (\Gamma_d - \Gamma)w'. \quad (12.15)$$

The air will be unstable (stable) if ΔT is positive (negative). Using (12.14), the stability criteria are

$$\begin{aligned} \frac{(\Gamma - \Gamma_s)}{(\Gamma_d - \Gamma)} &< \frac{A}{A'} && \text{stable,} \\ \frac{(\Gamma - \Gamma_s)}{(\Gamma_d - \Gamma)} &= \frac{A}{A'} && \text{neutral,} \\ \frac{(\Gamma - \Gamma_s)}{(\Gamma_d - \Gamma)} &> \frac{A}{A'} && \text{unstable.} \end{aligned} \quad (12.16)$$

It is of interest to examine the neutral condition. Since $A/A' > 0$, this condition requires that $\Gamma > \Gamma_s$. In the case of the parcel model, it is only necessary to have $\Gamma = \Gamma_s$ to be neutral. The new requirement implies that the compensating downdraft causes stabilization of the layer, and it requires a steeper lapse rate to make it unstable.

12.7 Brunt–Väisälä frequency

Oscillation is a general phenomenon of motion in a stably stratified fluid region such as at the surface of water. The layer around the LNB is also stably stratified and hence we expect to see oscillation here if the air at this level is disturbed. To see this, we note that the vertical equation of motion of the parcel under the influence of buoyant force (12.7) is

$$m \left(\frac{d^2 z}{dt^2} \right) = mg \left(\frac{\theta - \theta'}{\theta'} \right) \quad \text{or} \quad \frac{d^2 z}{dt^2} = g \left(\frac{\theta - \theta'}{\theta'} \right). \quad (12.17)$$

The quantity $(\theta - \theta')/\theta'$, which is a function of z , is much smaller than unity and can be expanded as

$$\left(\frac{\theta - \theta'}{\theta'} \right) = \left(\frac{\theta - \theta'}{\theta'} \right)_0 + \left[\frac{\partial}{\partial z} \left(\frac{\theta - \theta'}{\theta'} \right) \right]_0 z + \dots \quad (12.18)$$

The quantities with “0” subscript mean the values at the LNB. The first term on the right-hand side is zero because $\theta = \theta'$ at the LNB. The second term is

$$\left[\frac{\partial}{\partial z} \left(\frac{\theta - \theta'}{\theta'} \right) \right]_0 z = \left[\frac{\partial}{\partial z} \left(\frac{\theta}{\theta'} - 1 \right) \right]_0 z = - \left(\frac{\theta}{\theta'^2} \frac{\partial \theta'}{\partial z} \right) z \approx - \left(\frac{1}{\theta'} \frac{\partial \theta'}{\partial z} \right) z, \quad (12.19)$$

where we have used the fact that θ is constant because the parcel motion is adiabatic whereas θ' is not. Thus (12.17) becomes

$$\frac{d^2 z}{dt^2} = - \left(\frac{g}{\theta'} \frac{\partial \theta'}{\partial z} \right) z = -N^2 z, \quad (12.20)$$

where $N = \sqrt{(g/\theta')(\partial\theta'/\partial z)}$ (with unit s^{-1}) is called the *Brunt–Väisälä frequency* or *buoyant frequency*. Eq. (12.20) has the form of a wave equation and has general solutions of the form

$$z = A \exp(-iNt), \quad (12.21)$$

where A represents the wave amplitude. When N is positive, the solution (12.21) indicates that the parcel’s vertical position z oscillates with frequency N . Since a positive N implies that $(\partial\theta'/\partial z) > 0$, which indicates a stable stratification from (12.11), we naturally expect such oscillations to occur. On the other hand, if $(\partial\theta'/\partial z) < 0$, the stratification is unstable and N becomes imaginary. Eq. (12.21) then indicates that z will increase exponentially with time, i.e. the parcel accelerates away from the LNB, which is indeed what would occur in an unstable layer.

Such oscillatory motions generate *internal gravity waves* that can transport energy vertically. Even small cumulus clouds can induce internal gravity

waves, and a cumulonimbus will certainly generate such waves with larger amplitudes. Oscillatory motions near the overshooting dome of severe thunderstorms have been observed by radar and satellites, and have been successfully simulated by numerical thunderstorm models. We will discuss this in Chapter 15.

12.8 Convection process

The above discussions of air parcel thermodynamics and cloud formation are all based on the assumption that the motions are adiabatic. Whereas the adiabatic assumption is useful, it is admittedly only a crude approximation of the real cloud formation process. One of the most serious omissions is the mixing with environmental air because, after all, there is not really an impenetrable boundary between an air parcel and its environment, and velocity shears between them can easily cause mixing. Mixing has a great impact on cloud formation, especially convective clouds, and needs to be carefully examined.

12.8.1 Thermals and plumes

We used the concept of an air parcel in the above discussions as an abstract object without defining its size and shape. Since we will now discuss the interaction between the air parcel and the environment that eventually forms a cumulus, which does have finite size and shape, it is better for us to consider what that original air parcel looks like. There are three models for such air parcels (Fig. 12.5).

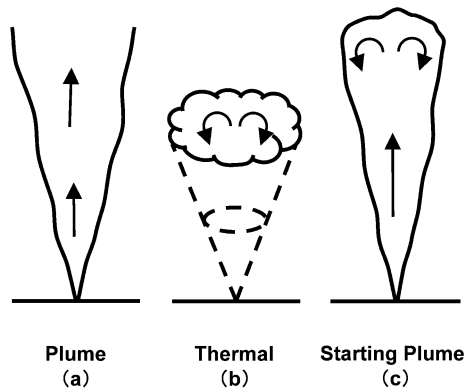


Fig. 12.5 Three convection models in the atmosphere: (a) plume; (b) thermal (bubble); and (c) starting plume. Adapted from Turner (1969).

- (a) *Plume* – a plume is a continuous column of ascending buoyant air that starts with relatively small diameter near the surface and expands as it goes up higher. The simplest plume model is one that expands upward at a constant angle. It has no top because it is assumed to be continuous.
- (b) *Thermal* – in this model, air parcels that eventually form cumulus are thought to be buoyant bubbles more or less spherical in shape. Glider pilots are familiar with the existence of such warm bubbles, which they call thermals. The thermals rise and interact with the environment and lead to the formation of Cu.
- (c) *Starting plume* – this model looks like a combination of the plume and thermal models. One can imagine that a thermal ascends first, and then successive thermals follow the same track as the first one, and eventually merge together to become a continuous plume but with a top that looks like a thermal.

A true continuous plume in the atmosphere is quite unlikely, so either the thermal or starting plume model is more realistic. However, the plume model is still mentioned from time to time due to its simplicity.

12.8.2 Lidar observations of thermals and small cumulus clouds

Before the formation of clouds, the thermals or plumes would be located in the boundary layer. Without the formation of clouds, they are basically invisible to the naked eye. However, the atmospheric boundary layer is usually full of aerosol particles, which, although invisible to the human eye, can be detected by lidar, as the particles backscatter strongly the incident laser beam. By recording the backscattered signal, lidar can “see” the structure of the boundary layer. The presence of thermals and plumes will influence the motions and concentrations of the aerosol. Thus, by examining the time evolution and space distribution of the aerosol backscattered profile, we can learn about the structure of the thermals and plumes.

Figs. 12.6–12.9 show four frames of a movie of the boundary layer evolution made by a volume imaging lidar on 27 July 1989 at Manhattan, Kansas. The top panel of each figure shows a vertical cross-section of the profile along the direction marked by the dashed line in the lower six panels. The lower six panels show the horizontal cross-sections of the backscatter field of $z = 250$ m, 500 m, 750 m, 1000 m, 1250 m, and 1500 m, respectively. Gray shades indicate aerosol, while brighter white shades indicate clouds.

Fig. 12.6 shows the backscatter fields at 9:37:46 a.m. Although it is relatively early in the morning, the boundary layer begins to build up as the ground begins to be heated. Convection cells start to be organized, although it is difficult to tell whether the cells are like bubbles or starting plumes from these images. The top panel shows

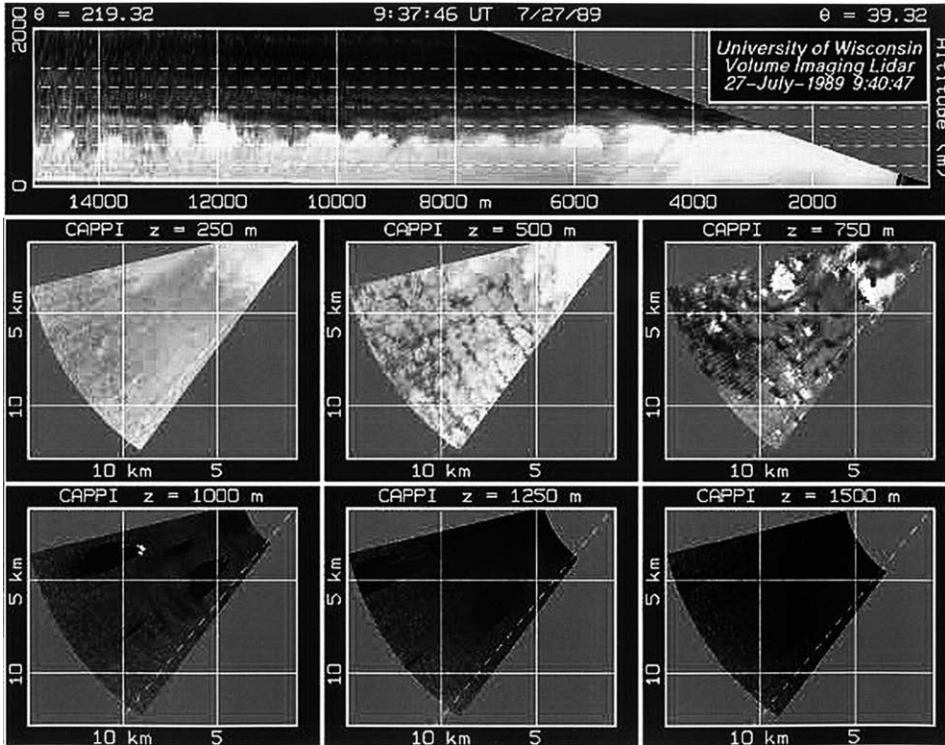


Fig. 12.6 Lidar observation of convection in the boundary layer at 9:37:46 a.m. on 27 July 1989 in Manhattan, Kansas. The top panel shows the vertical scan image. The lower six panels show horizontal scan images at $z = 250$ m, 500 m, 750 m, 1000 m, 1250 m, and 1500 m level. Gray objects are aerosol, while brighter white color represents clouds. Courtesy of Dr Edwin Eloranta.

the cell-like structure at the top of the boundary layer at z between 400 and 600 m. The middle figure in the middle panel ($z = 500$ m) shows the horizontal structure of this top layer, clearly indicating the cellular features with horizontal cell size ~ 500 m. At high level, for example, $z = 1000$ m, the atmosphere is relatively clean.

As time goes on, at 10:15:51 a.m. (Fig. 12.7), the boundary layer becomes thicker and the top of the layer pushes to a level between 800 and 1000 m. Some CCN at the top of the thermals are activated and small cumulus clouds begin to appear, as can be seen in the $z = 1000$ m panel (lower left). The fact that the clouds form directly on top of the thermals demonstrates that the thermals are indeed the “roots” of the clouds. The cellular structure below 500 m disappears but is still visible at $z = 750$ m. The cell size increases somewhat.

At 10:40:05 a.m. (Fig. 12.8), the boundary layer further thickens and the cloud top reaches a little higher than before. Cloud widths increase somewhat but cloud number becomes fewer, which is a quite common phenomenon in the development

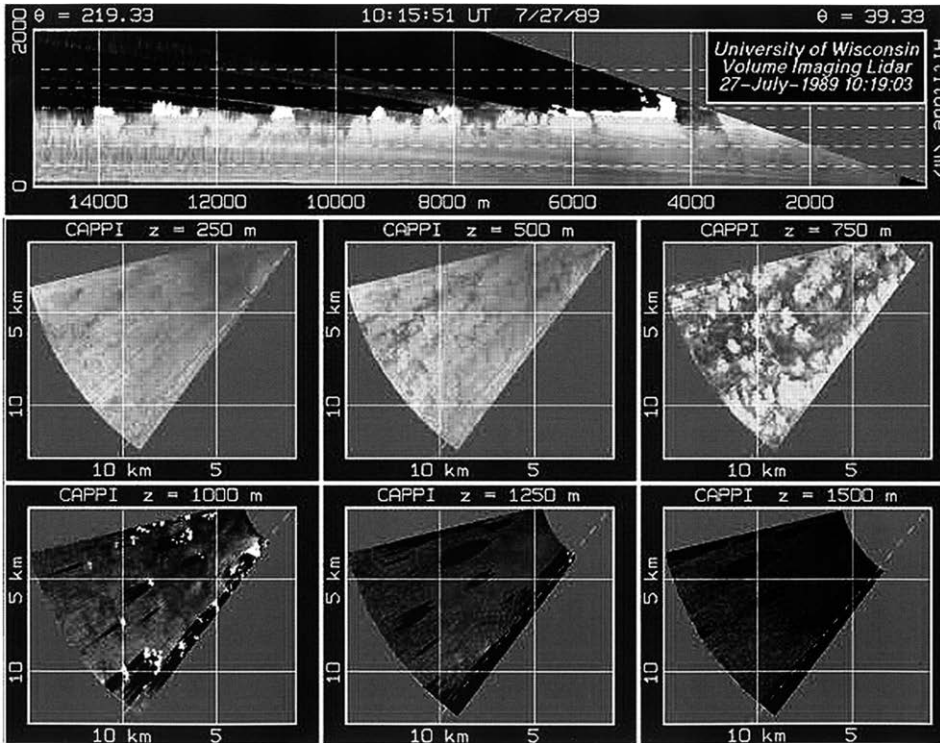


Fig. 12.7 Same as Fig. 12.6 except at 10:15:51 a.m. Courtesy of Dr Edwin Eloranta.

of a cumulus field in the morning. When some cloud cells grow taller, their more vigorous updrafts cause greater compensating downdrafts around them that may suppress the development of smaller clouds in that area. The net result is the decrease in number but an increase in size of the clouds. The cells at 500 m level remain more or less the same as in Fig. 12.6 but with somewhat larger size. Clouds are seen at the 1000 m level but not yet at the 1250 and 1500 m levels.

Fig. 12.9 shows the situation at 11:38:56 a.m., close to noon. The boundary layer thickness increases further and the top of the cloud now reaches 1500 m. Cloud widths also increase. The top panel shows that the clouds respond to the wind shear and tilt to the left. The aerosol field below 500 m appears to be well mixed, but the cellular structure can still be seen at the 1000 m level. Clouds can be seen in the 1250 and 1500 m scans.

12.9 Entrainment

The mixing between a rising air parcel and its environment is thought to be due to *entrainment*. Entrainment is especially important in the development of convective

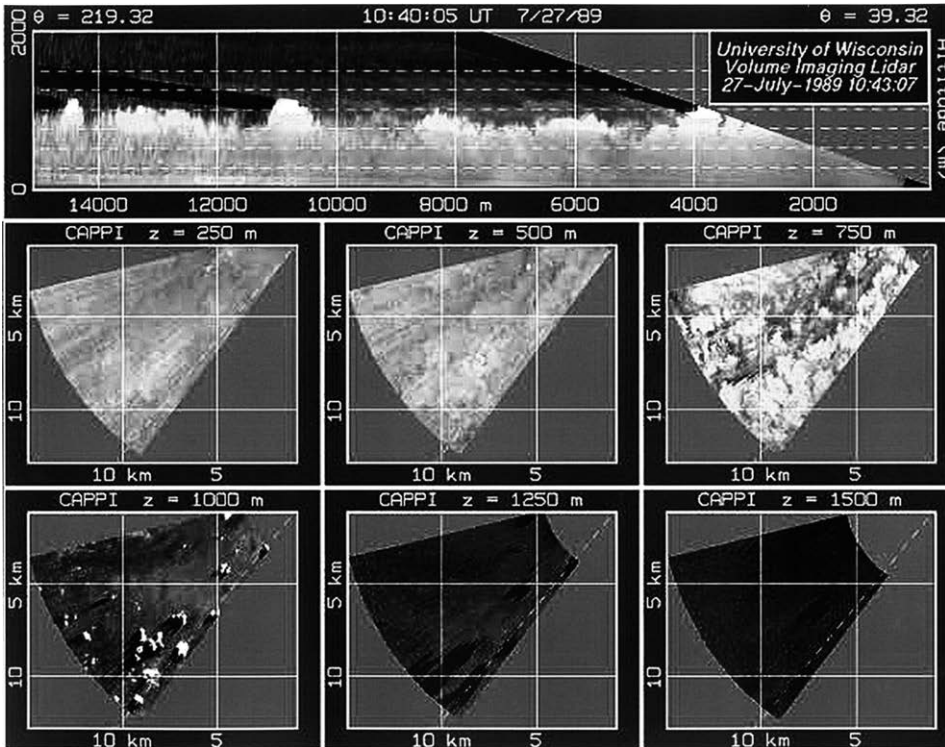


Fig. 12.8 Same as Fig. 12.6 except at 10:40:05 a.m. Courtesy of Dr Edwin Eloranta.

clouds because the larger updrafts of convective clouds tend to cause more vigorous mixing, and mixing changes the temperature and humidity profiles of the air parcel.

The fact that mixing does occur can be seen from the aircraft measurements of liquid water contents in cumulus clouds as depicted in Fig. 12.10. Here we see that the ratio of observed liquid water content (w_L) to that predicted by the pseudo-adiabatic theory ($w_{L,ad}$) is less than 1, indicating that cumulus cloud formation is never adiabatic. Furthermore, the ratio decreases with height, which implies that dilution due to entrainment becomes greater the higher in the cloud.

While the evidence for entrainment abounds, how entrainment occurs is much less clear and, in fact, is still debated to this date. In the following, we will examine some conceptual models of entrainment.

12.9.1 Lateral entrainment

The concept of entrainment was first introduced by Stommel (1947), and the idea was later adopted for the development of cumulus clouds by some cloud physicists (e.g. Scorer and Ludlam, 1953; Simpson, 1971). This idea is based on *lateral*

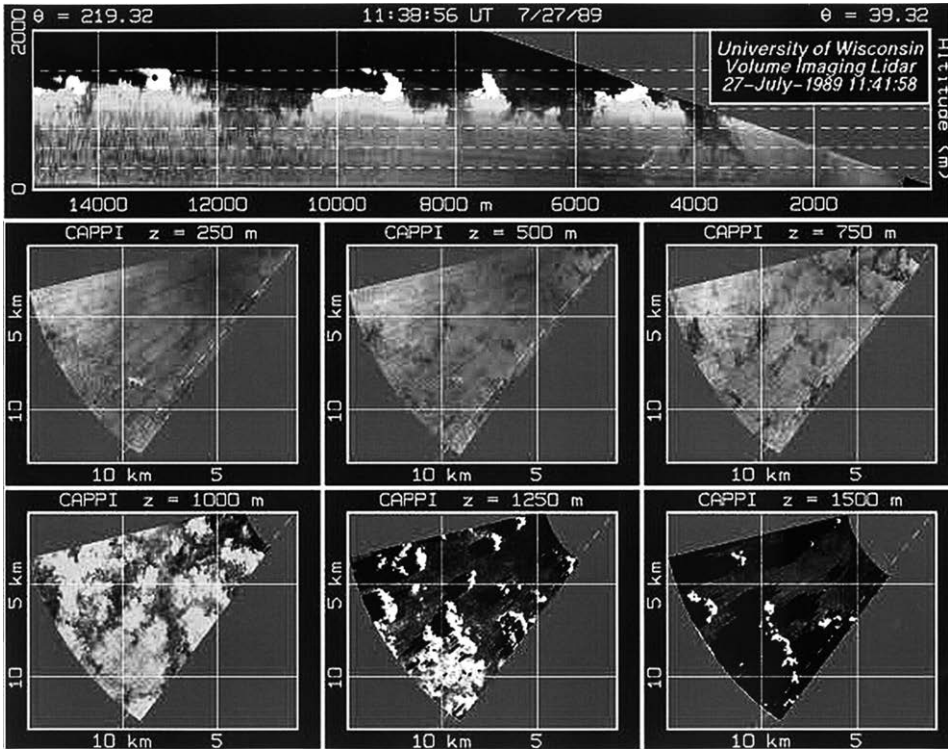


Fig. 12.9 Same as Fig. 12.6 except at 11:38:56 a.m. Courtesy of Dr Edwin Eloranta.

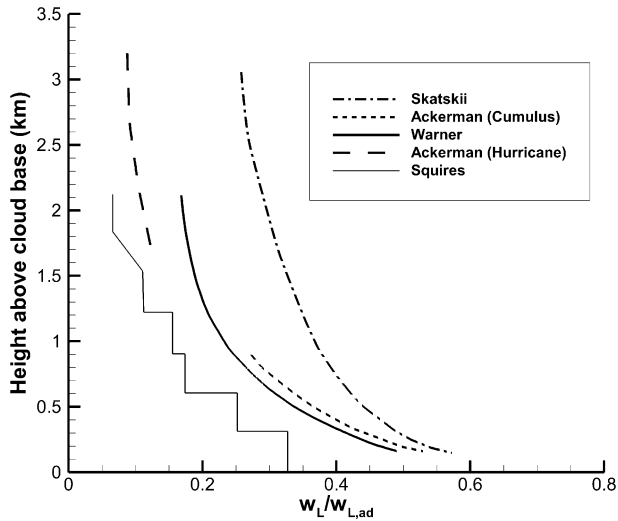


Fig. 12.10 The ratio of the observed mean liquid water content at a given height above cloud base to the adiabatic value. The values attributed to Skatskii (1965) were obtained from his published results assuming that the cloud base was at a height of 1 km and at a temperature of 8°C. Based on data from Warner (1970).

entrainment due to either plumes or bubbles (blobs). The lateral entrainment theory predicts that the fractional rate of entrained air into the cloud updraft varies with the cloud radius. This can be easily verified for the plume and thermal models. If we assume that a cloud system starts as a spherical bubble or thermal of radius r_B rising in a surrounding air environment, then the mass of the bubble is

$$m_B = 4\pi\rho_a r_B^3/3, \quad (12.22)$$

and hence the fractional entrainment rate is

$$\mu_B = \left(\frac{1}{m_B} \frac{dm_B}{dz} \right) = \frac{3(dr_B/dz)}{r_B} = \frac{C}{r_B}. \quad (12.23)$$

The term $dr_B/dz = C$ is constant because we assume that the bubble rises with a constant broadening angle.

Similarly, if the cloud starts as a continuous jet or plume with radius r_J , then the mass flux of the plume is given by

$$F_m = \pi r_J^2 \rho_a w, \quad (12.24)$$

where w is the updraft speed. Again, the fractional entrainment rate is

$$\mu_J = \left(\frac{1}{F_J} \frac{dF_J}{dz} \right) = \frac{2(dr_J/dz)}{r_J}, \quad (12.25)$$

where dr_J/dz is again constant for a fixed plume broadening angle.

If we take the bubble model result (12.23) and integrate, we obtain

$$\frac{dm_B}{dt} = \frac{dm_B}{dz} \frac{dz}{dt} = w \frac{dm_B}{dz} = \frac{C w m_B}{r_B} = C' \rho_a r_B^2 w, \quad (12.26)$$

where C' is just another constant. Eq. (12.26) predicts that the mass of entrained air is proportional to the cloud area and its updraft velocity. The properties of such entrainment processes have been measured in water tank experiments in the laboratory and then applied to the modeling of cloud development.

12.9.2 Cloud top entrainment

While the lateral entrainment model has the benefit of simplicity and is intuitively appealing, it also has many problems. Various observations have shown that pure lateral entrainment does not produce the right profile of liquid water content. For example, Warner (1970) found that the standard lateral entrainment model cannot correctly predict both the height of the ascending air parcel and the liquid water content at the same time when applied to a one-dimensional cloud model. In addition, it cannot explain the decreasing $w_L/w_{L,ad}$ with height, as shown in Fig. 12.10. There are also other discrepancies between the observations and the

predictions by the model. For example, Heymsfield *et al.* (1978) found undiluted air that originated from the cloud base at all levels in the cumuli. Paluch (1979) analyzed field observation data of cumuli in Colorado and showed that the entrained air at any observational level typically comes from a few kilometers above, and the mixed regions are typically found in downdrafts and weaker updraft regions. If the entrainment is lateral, the air should mostly come from below, instead of above, the observational level.

Another entrainment process was proposed by Squires (1958b) that is able to address these discrepancies. This is based on the concept that the entrainment mainly occurs at the cloud top by mixing. The action of this mechanism is the mixing of dry environmental air from above the ascending cloud top. Once the dry air is entrained into the cloud, it decreases the humidity and causes evaporative cooling. The result is that the air becomes colder than the surrounding cloudy air and sinks to lower level, causing the mixing effect. This is sometimes called the *penetrative downdraft model*.

Currently, both lateral and top mixings are considered in the more sophisticated numerical cloud models via parameterized forms.

Blyth *et al.* (1988) analyzed the data gathered by aircraft observations of small cumulus clouds in Montana. They concluded that cumulus clouds consist of thermal-like elements, from which the least buoyant mixed parcels are shed off and the most buoyant mixed parcels may continue with the general ascent. A more recent observation by Damiani *et al.* (2006) used airborne dual Doppler radar to study the velocity fields in vertical planes across cumulus turrets. They found clear evidence that the clouds evolved through a sequence of thermals with well-defined toroidal circulations (vortex rings). The largest updraft speeds were observed in the ring centers, but regions of turbulent ascending air extended behind the thermals to distances comparable with the toroid sizes. Patterns in the reflectivity and velocity fields indicated regions of major intrusions into the thermals, accompanied by entrainment of ambient air, or recycling of larger hydrometeors, depending on their location. In addition, at the upper cloud–environment interface, instability nodes contributed to further entrainment of cloud-free air. The findings of Damiani *et al.* (2006) largely confirmed the thermal shedding model proposed by Blyth *et al.* (1988).

12.9.3 Effect of entrainment on convective clouds

The net effect of entraining the colder and drier environmental air into the parcel is to reduce the buoyancy of the parcel so that the vertical velocity of the parcel is slower than that predicted by the adiabatic model. At the same time, the volume of the parcel becomes bigger due to the addition of the entrained outside air.

We can make a rough estimate of the influence on the parcel due to the entrainment. When the environmental air is entrained into the cloudy air parcel, it will expend an amount of heat $c_p (T - T')$ dm to warm up the colder new air, expend an amount $L_e (q_{v,\text{sat}} - q'_v)$ dm to evaporate some drops to saturate the drier new air, and, at the same time, gain an amount $L_e m dq_{v,\text{sat}}$ due to the latent heat released from condensation due to ascending cooling (which was already considered in the moist adiabatic process). The whole process is no longer adiabatic and therefore the conservation of energy now requires that

$$m \left(c_{p,a} dT + L_e dq_{v,\text{sat}} - R_a T \frac{dp}{p} \right) = c_{p,a} (T - T') dm + L_e (q_{v,\text{sat}} - q'_v) dm, \quad (12.27)$$

from which the lapse rate in a cloud with entrainment can be derived:

$$\Gamma_c = - \left(\frac{dT}{dz} \right)_c = \frac{g + \left(\frac{1}{m} \frac{dm}{dz} \right) [L_e (q_{v,\text{sat}} - q'_v) + c_{p,a} (T - T')]}{c_{p,a} + L_e (dq_{v,\text{sat}}/dT)}. \quad (12.28)$$

For an entraining cloud, the entrainment rate $\mu = (1/m)(dm/dz)$ is positive as well as the quantities in the square brackets. Thus, by comparing (12.28) with (12.5), we see that $\Gamma_c > \Gamma_s$, i.e. the lapse rate in an entraining cloud is greater than that of a pseudo-adiabatic cloud, as it should be because heat needs to be spent to warm up the colder air and evaporate some liquid drops.

12.10 Summary

What we have presented above are basic concepts of the dynamical processes for the formation of small cumulus clouds. The formulations are highly simplified so as to make them easy to understand and convenient for discussion. While useful, it is known that real cloud processes are much more complicated, and numerical cloud models are necessary to obtain more realistic and quantitative understanding of them. This is the subject of Chapter 13.

Problems

- 12.1 Prove that θ is conserved during a dry adiabatic process. Is θ conserved during a moist adiabatic process?
- 12.2 Prove that θ_e is conserved during a pseudo-adiabatic process. Is θ_e conserved during a dry adiabatic process?
- 12.3 Derive a set of stability criteria similar to (12.11) but using the wet-bulb potential temperature θ_w as the variable.